




Article

Sedimentary Ancient DNA Reveals Local Vegetation Changes Driven by Glacial Activity and Climate

Lucas D. Elliott ^{1,*} , Dilli P. Rijal ¹, Antony G. Brown ¹, Jostein Bakke ², Lasse Topstad ¹, Peter D. Heintzman ^{1,3,4}  and Inger G. Alsos ^{1,*} 

¹ The Arctic University Museum of Norway, UiT the Arctic University of Norway, 9006 Tromsø, Norway

² Department of Earth Science and Bjerknes Centre for Climate Research, University of Bergen, 5007 Bergen, Norway

³ Centre for Palaeogenetics, Svante Arrhenius väg 20C, 106 91 Stockholm, Sweden

⁴ Department of Geological Sciences, Stockholm University, 106 91 Stockholm, Sweden

* Correspondence: lucas.elliott@uit.no (L.D.E.); inger.g.alsos@uit.no (I.G.A.)

Abstract: Disentangling the effects of glaciers and climate on vegetation is complicated by the confounding role that climate plays in both systems. We reconstructed changes in vegetation occurring over the Holocene at Jøkelvatnet, a lake located directly downstream from the Langfjordjøkel glacier in northern Norway. We used a sedimentary ancient DNA (*sedaDNA*) metabarcoding dataset of 38 samples from a lake sediment core spanning 10,400 years using primers targeting the P6 loop of the *trnL* (UAA) intron. A total of 193 plant taxa were identified revealing a pattern of continually increasing richness over the time period. Vegetation surveys conducted around Jøkelvatnet show a high concordance with the taxa identified through *sedaDNA* metabarcoding. We identified four distinct vegetation assemblage zones with transitions at ca. 9.7, 8.4 and 4.3 ka with the first and last mirroring climatic shifts recorded by the Langfjordjøkel glacier. Soil disturbance trait values of the vegetation increased with glacial activity, suggesting that the glacier had a direct impact on plants growing in the catchment. Temperature optimum and moisture trait values correlated with both glacial activity and reconstructed climatic variables showing direct and indirect effects of climate change on the vegetation. In contrast to other catchments without an active glacier, the vegetation at Jøkelvatnet has displayed an increased sensitivity to climate change throughout the Middle and Late Holocene. Beyond the direct impact of climate change on arctic and alpine vegetation, our results suggest the ongoing disappearance of glaciers will have an additional effect on plant communities.

Keywords: *sedaDNA*; glaciers; vegetation reconstruction; climate change; Norway; Holocene



Citation: Elliott, L.D.; Rijal, D.P.; Brown, A.G.; Bakke, J.; Topstad, L.; Heintzman, P.D.; Alsos, I.G.

Sedimentary Ancient DNA Reveals Local Vegetation Changes Driven by Glacial Activity and Climate.

Quaternary **2023**, *6*, 7. <https://doi.org/10.3390/quat6010007>

Academic Editor: James B. Innes

Received: 1 November 2022

Revised: 17 December 2022

Accepted: 20 December 2022

Published: 7 January 2023



Copyright: © 2023 by the authors. Licensee MDPI, Basel, Switzerland. This article is an open access article distributed under the terms and conditions of the Creative Commons Attribution (CC BY) license (<https://creativecommons.org/licenses/by/4.0/>).

1. Introduction

Climate change affects both glaciers and arctic-alpine vegetation through variation in temperature and precipitation. However, glaciers can also have a more direct impact on alpine vegetation as they affect local climate, soil moisture, and soil disturbance [1]. Colonization of post-glacial landscapes is a heterogeneous process with many factors determining the resulting vegetation [2]. Early stages of succession in glacier forefields are largely controlled by geomorphic processes with the unstable, paraglacial landscape limiting vegetation to a few pioneer species [3] whereas later stages of succession are reliant on autogenic processes (e.g., plant colonization, chemical/physical weathering, and soil accumulation) [4].

After the Last Glacial Maximum (~20 thousand years ago, ka), during which northern Fennoscandia was almost completely covered by the Scandinavian Ice Sheet, large areas became ice-free 15 to 14 ka [5]. Deglaciation accelerated at the onset of the Holocene (11.7 ka) when temperatures quickly rose and the continuous ice sheet was broken up into valley/fjord glaciers, which became smaller or entirely absent by the Middle Holocene

(8.3 to 4.2 ka) [6–8]. Several abrupt cold events during this period caused the temporary readvancement or reformation of glaciers, but northern Fennoscandia was almost entirely glacier-free until the Late Holocene (4.2 ka to present) [9,10]. Many valley/fjord glaciers began to reform and underwent rapid fluctuations during the Late Holocene due to predominantly cool but variable temperatures [7,8].

Investigating past vegetation changes in response to a varying climate has been accomplished using pollen and macrofossils preserved in lake sediments [11,12]. However, several properties of pollen and macrofossils complicate the use of these proxies for vegetation reconstruction in the Arctic. The long-distance dispersal of pollen from certain wind-pollinated taxa (e.g., *Alnus alnobetula*, *Pinus sylvestris*) can present false positive signals of local taxa [13]. Many dominant arctic-alpine taxa rely on insect pollination (e.g., *Dryas*, *Saxifraga*) and their pollen is rarely detected in lake sediment records [14,15]. Both pollen and many macrofossils have limited taxonomic resolution and are unable to distinguish between many ecologically important taxa [16].

Studies using sedimentary ancient DNA (*sedaDNA*) have demonstrated how this technique overcomes many of the limitations of pollen and macrofossils [17]. *SedaDNA* provides a more localized vegetation signal limited to organisms found within the catchment of a lake [18]. Metabarcoding techniques targeting the trnL P6 loop region of the chloroplast genome, combined with a comprehensive local reference database, are able to identify a majority of vascular plant taxa from *sedaDNA* to below the genus-level [19,20]. The high taxonomic resolution and detectability of *sedaDNA* allows for taxa to be matched with trait value databases to provide a more in-depth and precise characterization of past vegetation communities [21,22].

Here, we investigate how the vegetation of Jøkelvatnet changed in relation to the Langfjordjøkelen glacier over the Holocene using *sedaDNA* metabarcoding data together with glacial activity and climatic reconstructions. We examine a subset of the data from [22] and offer a detailed reconstruction of the vegetation and new analyses addressing the causes of observed vegetation changes. Vegetation composition is described using ecological indicator trait values from [21] and compared to both reconstructions of Langfjordjøkelen's glacial activity [23] and regional climate reconstructions [24] to enhance our knowledge of how climate affects plants directly (temperature and precipitation) and indirectly through glaciers (soil disturbance).

2. Materials and Methods

2.1. Study Site

Jøkelvatnet (70°10'21" N 21°42'3" E at 158 m a.s.l.) is a distal glacier-fed lake located in northern Norway in the valley of Sør-Tverrfjorddalen (Figure 1), immediately downstream from the 7.49 km² Langfjordjøkelen ice cap [25]. The surface area of the two-basin lake is ~0.13 km² with the deepest part located in the southern basin at ~10 m water depth [23]. The lake's catchment area is ~11 km² with 18% currently covered by the ice cap and the remainder primarily composed of talus slopes and steep mountain ridges (Figure 1, [23]). The Sør-Tverrfjorddalen valley was completely deglaciated from 10.0 ka until the glacier reformed at 4.1 ka with large fluctuations in glacial activity over the last two millennia [23]. The valley lies in the Caledonian province of Finnmark and is underlain by allochthonous felsic igneous and metamorphic rocks particularly gabbro and amphibolites. However, the valley floor and gentler slopes are covered by glacial deposits including moraines, till (diamicton) and screes. These deposits have a broader clast lithology which includes sands and gravel with clasts of gneiss, psammite and gabbro. The gabbro and amphibolites are highly fractured and in places highly weathered, producing regoliths and thin soils that have a relatively high nutrient index (high-moderate Mg and Ca) sensu [26].

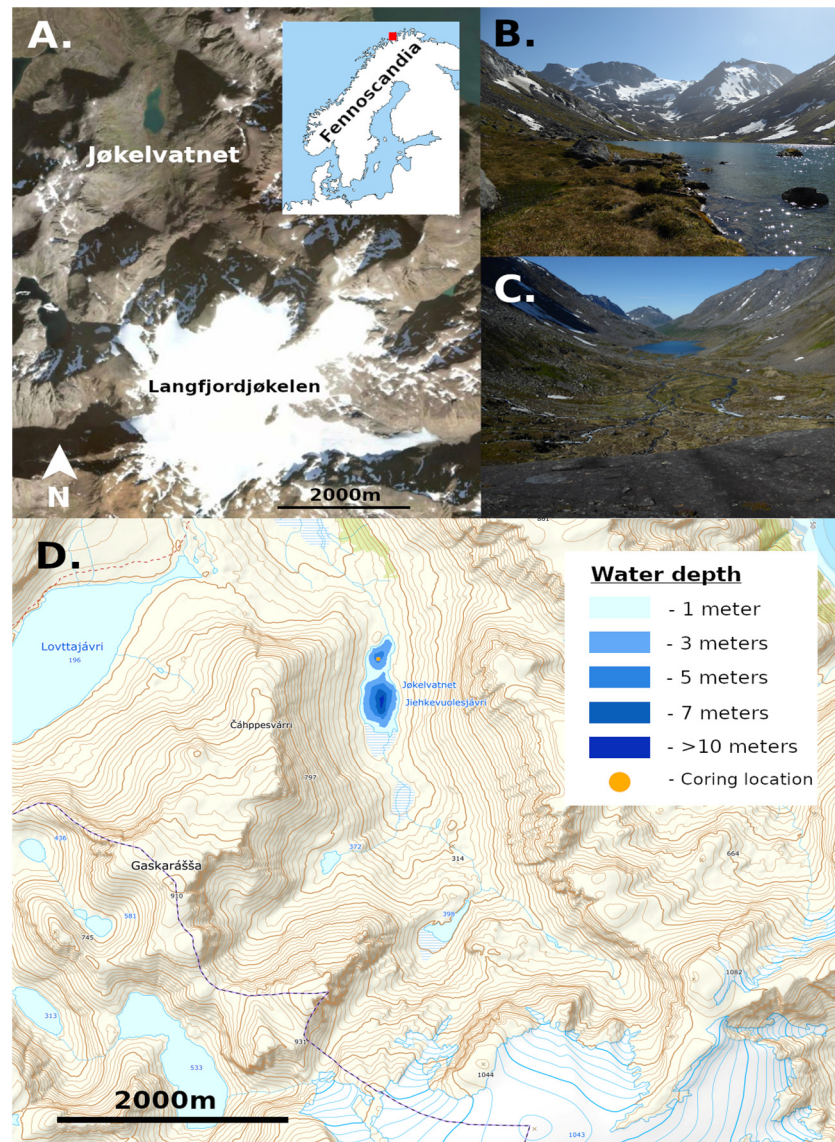


Figure 1. (A) Satellite image (norgeskart.no accessed 29 April 2022) of Lake Jøkelvatnet and the Langfjordjøkelen glacier with inset map of Fennoscandia. (B) View looking south towards the glacier from the northern outlet of the lake. (C) View looking north over the lake from near the glacier. Photographs taken by I. G. Alsos in July 2021. (D) Topographic map (norgeskart.no) of the catchment and lake bathymetry showing the coring location of JØP-112.

2.2. Vegetation Surveys

Two vascular plant surveys were conducted in the Sør-Tverrfjorddalen valley with a focus on the catchment of Jøkelvatnet during September 2020 and July 2021. For both surveys, we aimed to record all taxa growing within 2 m of the lake shore and efforts were made to identify taxa growing in the various habitats further upslope. Herbarium vouchers were collected for most taxa and deposited in the herbarium at Tromsø museum. Data from both vegetation surveys was compiled into one dataset consisting of all taxa observed in the catchment.

2.3. Coring, Age-Depth Model, and Stratigraphy

Two piston cores [27] were retrieved from the northern basin of Lake Jøkelvatnet (Figure 1D) in March 2012 and stored at 4 °C until opening [23]. The shielded northern basin was chosen for coring in order to avoid potential disturbances from the main inlet delta in

the south. One 258 cm core (JØP-112) was split longitudinally and a total of 40 sediment samples spaced ~7 cm apart, were collected in the clean labs of GeoMicrobiology at the Department of Earth Science, University of Bergen, Norway for sedaDNA analysis as described in [26]. A Bayesian age-depth model was constructed by [22] using Bacon v2.3.4 [28] and the IntCal13 calibration curve [29] using 12 radiocarbon (^{14}C) dates from plant macrofossils found throughout the core [23]. Five samples fell below the basal-most radiocarbon date so extrapolation of the model was explored using different accumulation rate priors and correlating unit transitions with Lake Stortvatnet (STP-112) located 5 km downstream in the same valley [22]. No signs of redeposition were detected and full details of the age-depth model construction of JØP-112 can be found in [22]. The core stratigraphy is a basal unit of dark-gray silty clay with some banding but low organic matter content. Above this is strongly laminated dark gray to olive-gray silty gyttja with a moderate organic matter content (6%). The upper 128 cm are variable generally laminated olive-gray and brown-gray silty clays with frequent visible plant remains but low loss on ignition values (2–6%). More details of the core lithostratigraphy can be found in [23].

2.4. *sedaDNA* Data Generation

sedaDNA sampling, extraction, amplification, and sequencing steps were described in [22,26] and are summarized here. DNA was extracted from 0.25 to 0.35 g of sediment for each sample using a modified version of the Qiagen DNeasy PowerSoil PowerLyzer (Qiagen Norge, Oslo, Norway) protocol. Six negative controls (composed of water exposed during sediment sampling, extraction, or PCR plating) and one positive PCR control were processed in addition to the 40 samples. DNA was amplified using the “gh” primer set which targets the vascular plant *trnL* p6-loop locus of the chloroplast genome [19]. The gh primers were uniquely dual-tagged with an 8 or 9 base pair tag, modified from [30]. Eight PCR replicates were amplified for each sediment sample and control DNA extract in a post-PCR laboratory located in a different building from the ancient DNA lab facility at The Arctic University Museum of Norway. Two DNA libraries of these amplicons were prepared using a modified Illumina TruSeq DNA PCR-Free protocol (Illumina Inc., CA, USA) with unique dual indexes, while the magnetic bead cleanup steps were modified to retain short amplicons. The two libraries were sequenced on ~10% of 2x 150-cycle mid-output flow cell on the Illumina NextSeq platform at the Genomics Support Centre Tromsø at The Arctic University of Norway.

2.5. Bioinformatics

The *sedaDNA* dataset presented here is a subset of the filtered data presented in [22]. The initial bioinformatic pipeline incorporates OBITools [31] and custom Python and R scripts to filter the data following [26]. Briefly, paired-end reads were merged using SeqPrep (<https://github.com/jstjohn/SeqPrep/releases>, v1.2 (accessed on 26 September 2022)) and then demultiplexed to individual samples using their 8 base pair tags, followed by the collapsing of identical reads. PCR artifacts were filtered using OBIClean and potential library swaps were corrected using a custom Python script (<https://github.com/Y-Lammers/MetabarcodingFilter> (accessed on 26 September 2022)). For each PCR replicate, sequences with ≤ 2 reads were discarded. Sequences represented by fewer than 10 reads or three PCR replicates in the entire regional dataset were also removed [22]. Sequences were then matched to the following four databases: (1) PhyloNorway [22], (2) a combination of 815 arctic [32] and 835 boreal [33] vascular plant taxa and 455 arctic-boreal bryophytes [34] from the circumpolar region (ArcBorBryo, $n = 2280$ sequences of which 1053 are unique), (3) PhyloAlps ($n = 4604$ specimens of 4437 taxa collected in the Alps and Carpathians, [35] (<https://data.phyloalps.org/browse/> (accessed on 26 September 2022)), and (4) EMBL (release 143, $n = 159,748$ sequences of 74,936 taxa). Sequences with a 100% identification match to at least one taxonomic reference database were retained. Sequences assigned to the same taxon were merged by combining their read counts and taking the maximum number of PCR repeats the sequence was found in at each sample depth. The final taxonomic

assignment of the retained species was determined using regional botanical taxonomic expertise by Alsos and following the taxonomy of the Panarctic Flora [36] and Lid's Norsk Flora [37]. All taxa identified in the negative controls were discarded from the overall dataset. Sample quality was assessed using the metabarcoding technical quality (MTQ) and metabarcoding analytical quality (MAQ) scores, which, respectively, measure overall metabarcoding success and the success of retrieving barcodes of interest, following the approach of [26].

2.6. Data Analysis

All further data filtering, analysis, and plotting was performed using custom Python and R scripts (https://github.com/salanova-elliott/jokelvatnet_data (accessed on 26 September 2022)) using the *vegan* [38], *rioja* [39], and *ggplot2* [40] packages. To compare the compositional changes of the vegetation communities through time, we used a stratigraphically constrained sum of squares (CONISS) cluster analysis (Grimm 1987) with a broken stick model to determine the number of statistically significant clusters. We performed this analysis both using the proportion of PCR replicates that a single taxon appears in per sample and using the proportion of total retained reads that taxon appears in per sample. The results of both analyses are presented here, but we focus on the proportion of PCR replicates since this measure is considered to more clearly reflect community composition changes. Vascular plant taxa were assigned ecological trait values from [21] for the following traits: moisture (12 degree scale), temperature optimum (18 degree scale), and soil disturbance (9 degree scale). These traits were selected as those most likely to be influenced by climate and glacial activity. The temperature optimum index was inverted to provide for a more intuitive interpretation (1 = high alpine/arctic taxa, 18 = subtropical taxa). The assignment of traits to genus- or family-level identifications follows those described in [22]. Briefly, average trait values for all corresponding taxa present in the region today were averaged if within <3 category differences for soil disturbance, <4 for moisture, <5 for temperature optimum. These values were averaged and weighted on PCR replicates for each sample to produce a single value for each trait.

Reconstructed climatic data for Jøkelvatnet was retrieved from the CHELSA-TraCE21k model [24] using a custom python script (https://github.com/salanova-elliott/chelsa_retrieve (accessed on 26 September 2022)) using the coordinates 70.1715 N, 21.7014 E. We specifically examined the variables "mean temperature of warmest quarter" (bio10) and "annual precipitation" (bio12). Summer temperatures were used instead of annual temperatures since arctic flora are more responsive to changes during their growing season [41]. Values for specific years were linearly interpolated from the 100 year resolution climate data. Ti (cps) was used as a proxy for glacial activity in the catchment as presented by [23]. We used simple linear regressions to explore the relationship between the average weighted trait values, glacial activity, and the reconstructed climatic variables.

3. Results

3.1. *sedDNA* Dataset Composition

The 8 PCR replicates of 40 samples and 6 controls produced a total of 8,551,653 reads (mean of 198,026 per sample). We retained 38 samples that had a metabarcoding technical quality (MTQ) score > 0.75 (mean of 0.970, $\sigma = 0.055$) and a metabarcoding analytical quality (MAQ) score > 0.2 (mean of 0.918, $\sigma = 0.146$). All 6 control samples had MTQ and MAQ scores below these thresholds. From the initial 8.5 million reads, ~65% passed quality filtering and were assigned with 100% identity to a taxon. Post-identification filtering resulted in a final dataset of 193 taxa composed of 25% identified at the family-level or above, 26% at genus-level, and 49% at species-level. Of these 193 taxa, 133 are the targeted vascular plant taxa, with 16% at the family-level, 32% at genus-level, and 52% at species-level while the other 60 are bryophytes. We note that some of the identifications considered at genus- and family-level in the aforementioned statistics can be confidently resolved to a subset of lower taxa (e.g., *Ranunculus glacialis/hyperboreus* is considered genus-level despite

being narrowed down to two out of 24 potential regional species of *Ranunculus*). Two algal taxa were not included in the final dataset as their presence does not reflect terrestrial vegetation changes and their identification is strongly limited by a lack of representation of algae in the reference library.

3.2. Zonation

A stratigraphically constrained cluster (CONISS) analysis performed on the proportion of PCR replicates assigned to each taxon and compared with a broken stick model suggests the presence of four statistically significant zones in the data. The analysis performed on the read count data provided the same number of zones, with some slightly shifted boundaries (Figures S1 and S2; the oldest zone boundary changes by one sample from 9.7 ka to 9.6 ka, while the middle boundary also changes by one sample from 8.4 ka to 8.0 ka). The nearly identical zone boundaries identified by CONISS using proportion of PCR replicates and proportion of total reads support the interpretation of concurrent increases in taxonomic richness and changes in taxonomic abundance during each zone transition. The full data for each growth form are in Figure S3, whereas the pattern of abundance and richness for each growth form for these zones are displayed in Figure 2A,B.

The vegetation changes throughout the Holocene have largely coincided with changes in glacial activity, as inferred by changes in Ti count rates throughout the sediment core. The major boundary identified by CONISS at ~8.4 ka is at a time with high arrival of new taxa, especially forbs (Figure S3). The other two boundaries identified by CONISS coincide with major turning points in glacial activity identified by [23]. The boundary at ~9.7 ka occurs shortly after the valley becomes entirely deglaciated at 10 ka. The boundary division at ~4.3 ka occurs just prior to the onset of the Late Holocene as the Langfjordjøkelen ice cap begins to reform (Figure 2).

3.2.1. Zone 1

10.4–9.8 ka (4 samples). This zone is characterized by relatively few taxa per sample (mean of 16.8, $\sigma = 6.4$) and was dominated in read counts by Saliceae. These Saliceae likely include cold tolerant dwarf shrubs as *Salix herbacea*, *S. reticulata*, and *S. polaris*, which were identified in the vegetation survey close to the present glacier. Bryophytes (*Grimmiaceae*), ferns (*Cystopteris*, *Woodsia*), forbs (*Bistorta vivipara*, *Oxyria digyna*, *Saxifraga oppositifolia*, *Bartsia alpina*), and some dwarf shrubs (*Dryas octopetala*, *Empetrum nigrum*) were also present.

3.2.2. Zone 2

9.7–8.7 ka (5 samples). A dramatic decrease in the read proportion of Saliceae, as well as the appearance of additional woody taxa *Betula* and *Sorbus aucuparia*, occurred at the start of this zone. The arrival of *Athyrium* and *Phegopteris connectilis* caused a large spike in the read proportions of ferns (Figure 2A). Taxonomic richness continued to increase over this zone (mean taxa per sample of 26.6, $\sigma = 4.6$) with 18 new forb taxa arriving (Figure 2B).

3.2.3. Zone 3

8.2–4.5 ka (9 samples). Taxonomic richness sharply increased at the start of this zone (mean taxa per sample of 57.4, $\sigma = 8.5$). Dwarf shrubs such as *Vaccinium myrtillus*, *Vaccinium vitis-idaea*, *Phyllodoce caerulea*, as well as *Empetrum nigrum*, were responsible for the rise in the read proportions of dwarf shrubs while Saliceae and tree species also increased (Figure 2A).

3.2.4. Zone 4

4.2–0 ka (20 samples). This zone begins with another sharp increase of taxonomic diversity (mean taxa per sample of 86.2, $\sigma = 12.8$) with 67 taxa found only in this period. Graminoids in particular became more diverse with 12 new taxa after being composed primarily of *Oreojuncus trifidus* in the previous two zones. Bryophytes and forbs showed an

increase in diversity as well, with large fluctuations in total taxonomic richness throughout the zone (Figure 2B). Saliceae makes up >50% of the total read proportion for the majority of this zone (Figure 2A) which likely includes the pioneer species mentioned in Zone 1, but also the shrub-forming *Salix phylicifolia* growing near the lake.

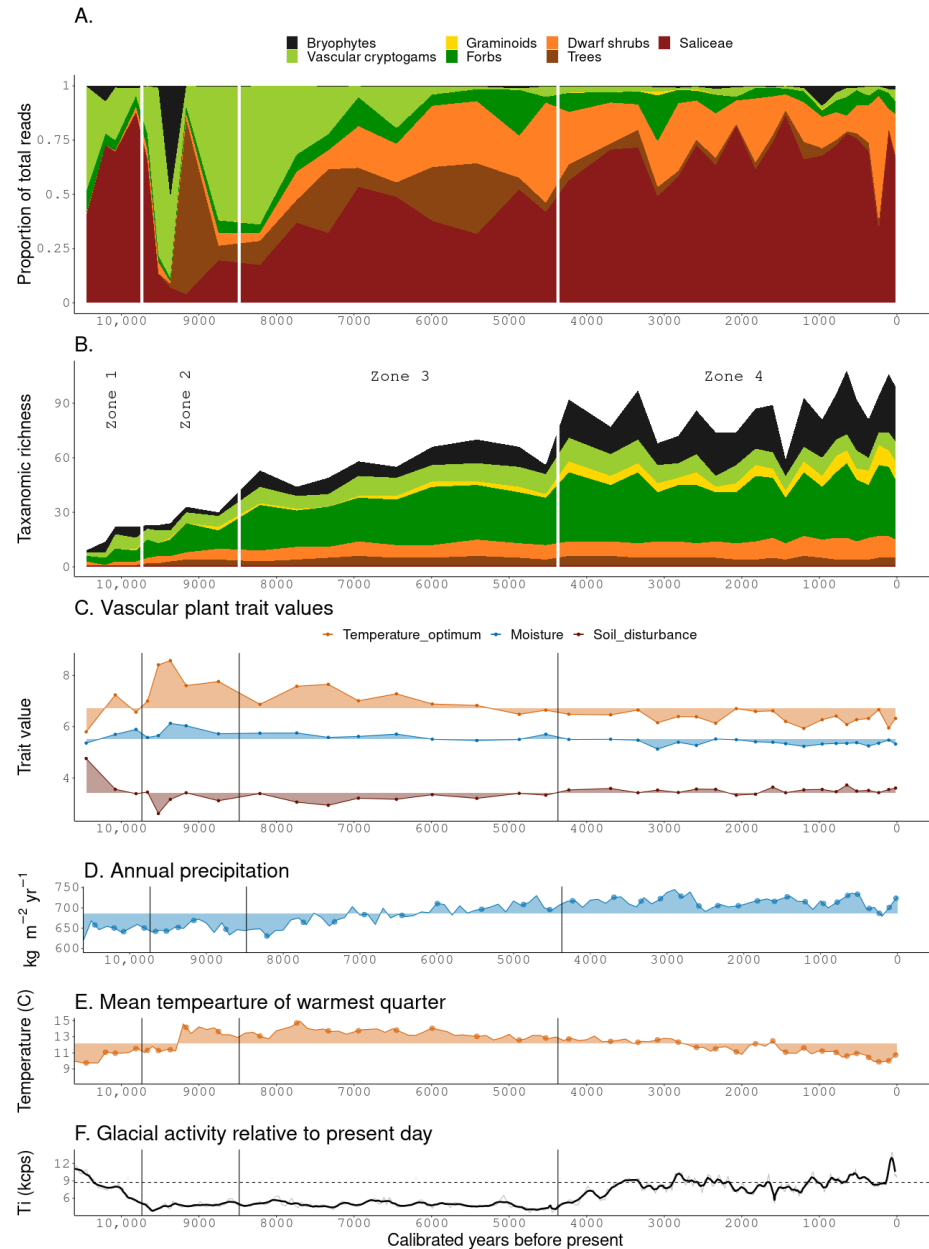


Figure 2. An overview of *sedaDNA* results, climate reconstructions, and glacial activity. CONISS zone boundaries are demarcated with vertical bars at 9.7, 8.4, and 4.3 ka. (A) Proportion of total identified reads by plant functional group. (B) Stacked taxonomic richness for each functional group. (C) Average weighted vascular plant trait values are based on plants identified in the *sedaDNA* combined with plant trait values reported in [21]. Note that temperature optimum index values are inverted from those reported in [21]. High values indicate high temperature optimum, high moisture requirement and high dependents of soil disturbance. (D) Annual precipitation data (bio12) from [24]. Points represent the age of samples taken from the core. (E) Mean temperature of the warmest quarter (bio10) from [24]. Points represent the age of samples taken from the core. (F) Glacial activity relative to the present day (dashed horizontal line) adapted from [23].

3.3. Ecological Trait Values

From the eligible 133 vascular plant taxa, 90 taxa were found to have informative ecological trait values for “soil disturbance”, 81 taxa for “moisture”, and 74 taxa for “temperature optimum”. The second oldest sample at 10.2 ka had <5 taxa for each trait examined, and was consequently excluded from the trait analyses. The average soil disturbance index of the plant community starts at a high value of 4.7 (5 = requires soil disturbance for reproduction, but established individuals may persist for long (decades–centuries) in undisturbed vegetation), and then decreases to a low value of 2.6 (2 = colonizes already established vegetation, successfully competes with for some time but in the long run out-competed if there is no soil disturbance) at 9.5 ka (Figure 2C). This value then gradually increases while approaching the present at 3.6 (4 = with some capacity to reproduce also in undisturbed established vegetation, but not sufficient to keep a stable population size). The temperature optimum index follows an inverted trend of this pattern with an initial dominance of cold-adapted plants, increasing temperature optimum values in zone 2 with a peak of 8.6 at 9.3 ka, and then colder taxa gradually become more prevalent towards the current day (Figure 2D). The average moisture trait values show a similar trend on a smaller scale where values peak at 6.1 (6 = moist) at 9.3 ka and then erratically decrease approaching the present day with a minimum value of 5.1 (5 = mesic-moist) at 3.1 ka (Figure 2E). The spike in average moisture trait value at 9.3 ka can be attributed to the temporary disappearance of the “dry-mesic” (moisture trait value = 3) *Cryptogramma crispa* and *Arctous alpina* as well as the appearance of the “moist-wet” *Bartsia alpina* (moisture trait value = 7). The appearance of many “mesic” (moisture trait value = 4) graminoids (*Oreojuncus trifidus*, *Avenella flexuosa*, and *Poa pratensis / alpina / Anthoxanthum*) and forbs (*Diapensia lapponica* and *Ranunculus acris / subborealis*) in the Late Holocene causes the average moisture trait value to decrease through this time period.

3.4. Taxonomic Persistence and Vegetation Surveys

We identified 109 taxa in the combined vascular plant survey, of which 101 are represented in the metabarcoding data (Table S1). From the 133 vascular plant taxa present in the metabarcoding data, 108 were represented across both vegetation surveys (Table S1). The discrepancy between taxa counts of the two measures is due to the differing level of taxonomic identification in the vascular survey compared to metabarcoding (e.g., four *Salix* species were identified in the vascular plant survey whereas metabarcoding can only resolve the tribe Saliceae). The remaining 25 taxa in the metabarcoding dataset were not observed during either vegetation survey despite a directed effort to locate them during our second survey. However, 17 of these taxa were not found in the most recent metabarcoding samples, while 11 appear in ≤ 2 samples suggesting that they may no longer grow in the catchment or are very rare. In contrast, the majority of taxa persisted from one zone to the next, with 94%, 97%, and 96% of taxa detected in zone 1, 2, and 3, respectively, also detected in zone 4 (Figure 3). The few taxa that disappear in the record are bryophytes or forbs that appear in only one sample with <4 replicates.

The vegetation survey revealed that the large floodplain at the inlet in the south end is dominated by *Eriophorum angustifolium* and *Salix herbaceae* with smaller patches of *Nardus stricta* and *Deschampsia cespitosa* and a near 100% bryophyte layer largely composed of *Sphagnum*. The majority of the vegetation 10–20 m from the lake shore is Alpine heath dominated by *Empetrum nigrum*, *Vaccinium myrtillus*, *Phyllodoce caerulea*, with the sedge *Carex bigelowii* being co-dominant. Slopes surrounding the lake are dominated by tallus with two small patches of *Betula pubescens* forest located on the north-west slopes of the lake. There were several springs in the hillslopes, one of them very rich with *Angelica archangelica* and *Anthriscus sylvestris*. Moraines towards the current glacier have discontinuous cover of typical arctic-alpine species as *Dryas octopetala*, *Kalmia procumbens* and *Ranunculus glacialis*.

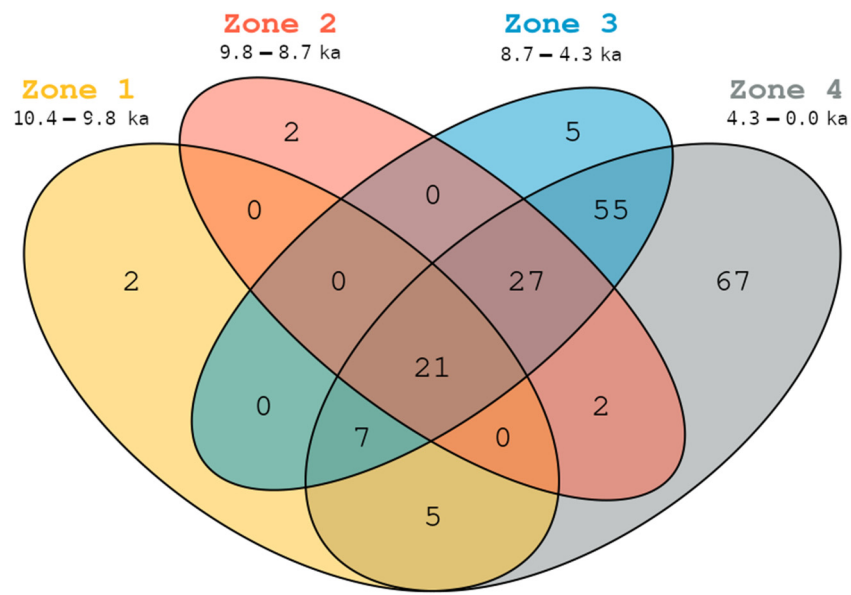


Figure 3. Number of plant taxa identified in the *sedaDNA* analyses that are shared between CONISS demarcated zones.

3.5. Linear Regressions

Soil disturbance, temperature optimum, and moisture values show a significant and intermediate strong correlation with glacial activity ($p < 0.001$, $R^2 \approx 0.4$; Figure 4). Two samples (9.4 and 9.5 ka) were identified as outliers and removed for linear regressions involving the temperature optimum trait value. These samples occur directly before the spike in summer temperatures reconstructed by CHELSA at 9.3 ka. Plant traits for temperature optimum show a significant correlation with the mean temperature of warmest quarter (bio10) data from CHELSA-TraCE21k ($p < 0.001$), with more cold tolerant plants present when the mean temperature is lower (Figure 5). Moisture trait values show a similar, but inverted, correlation with annual precipitation (bio12) data ($p < 0.001$) where dry-adapted plants become more prevalent as precipitation increases (Figure 5). Samples from early in the record have fewer taxa present and display more variability, but still largely follow the described trends (Figures 4 and 5).

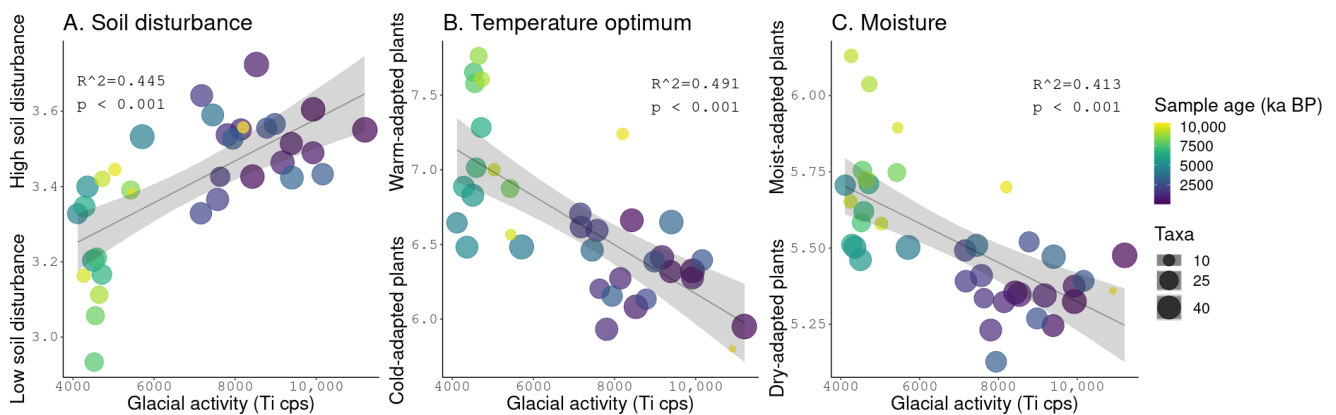


Figure 4. Linear regression of glacial activity and (A) soil disturbance, (B) temperature optimum, and (C) moisture trait values based on plants identified in the *sedaDNA* combined with plant trait values reported in [21]. The number of plant taxa used to calculate the weighted average is shown as point size while sample age is represented as a color scale. Note that temperature optimum index values are inverted from those reported in [21].

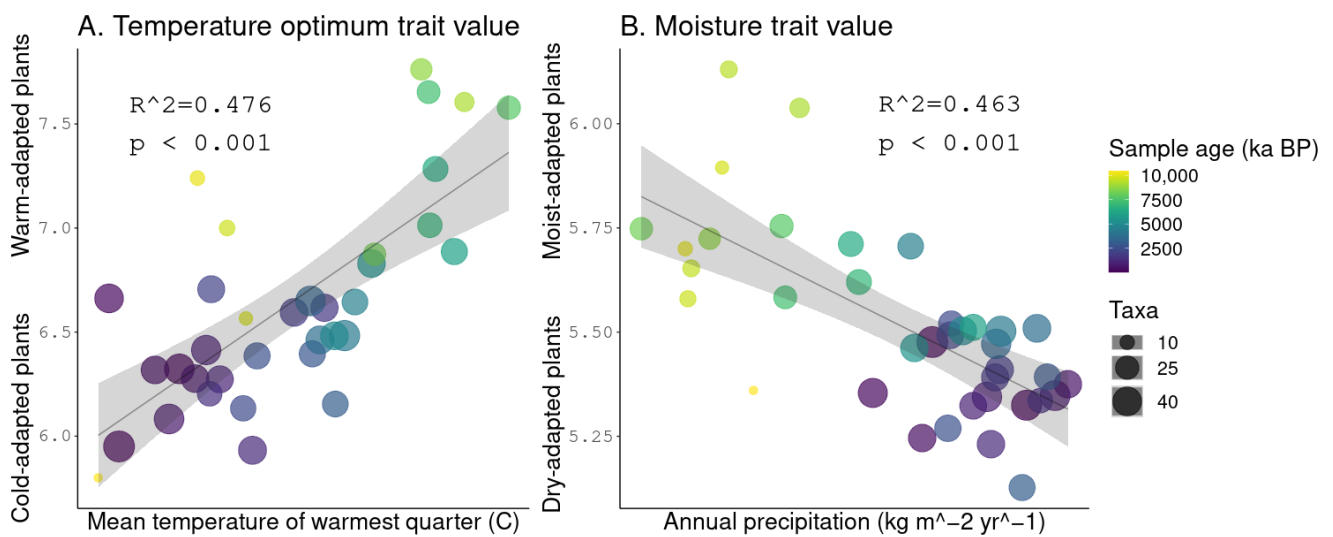


Figure 5. Linear regression of (A) the mean temperature of the warmest quarter and the temperature optimum trait value and (B) the annual precipitation and moisture trait value. The number of plant taxa used to calculate the weighted average is shown as point size while sample age is represented as a color scale. Note that temperature optimum index values are inverted from those reported in [21].

4. Discussion

Our study shows shifts in both species richness and composition coinciding with changes in glacial activity. A number of other studies have used metabarcoding to examine vegetation changes in a lake catchment containing an active glacier [42–44], but few offer direct analogues to Jøkelvatnet’s system of near-complete glacial melting followed by significant reformation during the Late Holocene. With nearly one fifth of the catchment currently occupied by the glacier, vegetation changes as a result of the glacier’s influence are readily apparent in the *sedaDNA* record. In contrast to pollen’s long dispersal distances, *sedaDNA* represents a local signal of taxa growing in the catchment [17,18]. Compared to the overall pattern found across ten lakes in northern Fennoscandia, Jøkelvatnet stands out by showing more variation during the Middle to Late Holocene in plant trait values, when the overall pattern of the region is a more stable ecosystem [22]. Here, we posit that the presence of the Langfjordjøkel glacier enhances the effects of Holocene climate change on the vegetation in the catchment.

The overall trend of increasing taxonomic richness throughout the Holocene at Jøkelvatnet is consistent with other lake catchments across northern Fennoscandia [26]. At Jøkelvatnet, the taxonomic richness at each timepoint is increasing at a consistent rate from the beginning of the record until 4.2 ka when it begins to fluctuate dramatically (Figure 2B). This could reflect the rapidly changing landscape of the Late Holocene period where the Langfjordjøkel ice cap is repeatedly reforming and melting. In contrast to expectations of increased soil erosion delaying succession sequences [1], taxonomic richness increased even during periods of high erosion (Figure 2B). In other lake catchments, an influx of glacial flour has been documented as coinciding with a decrease in overall DNA concentration in the sediment, but this decrease is not necessarily reflected in the number of MOTUs retrieved from these periods [43]. Since the vegetation here is recorded from the entire catchment, new taxa are able to colonize the disturbed soils near the glacier as well as the later successional environments at the eastern and western slopes of the lake.

There are only nine taxa that appear in the record and then disappear entirely in subsequent zones (Figure 3). Many of these taxa are bryophytes that are present in only one sample with few PCR replicates (Figure S4) suggesting a low abundance in *sedaDNA* and/or difficulty in detection. The detectability of plants is related to their abundance in the catchment [45], and bryophytes in general show less consistent detection than vascular

plants [22,46]. Thus, similar to observations for the region of N Fennoscandia [22], we assume that local extirpation has been low in this catchment.

The average temperature optimum trait value's correlation with glacial activity (Figure 5) is in accordance with [23]'s observation of Langfjordjøkelen's glacial activity following regional summer temperatures. Vegetation temperature optimum values at the beginning of the core reflect the relatively rapid warming of the Early Holocene (Figure 2D). Communities of high arctic/alpine taxa are supplemented with warmer taxa at the beginning of the Holocene Thermal Maximum at ~9.5 ka. An increased abundance of cold tolerant forbs and dwarf shrubs (*Oxyria digyna*, *Dryas octopetala*, *Kalmia procumbens*) causes a small dip of cold temperature optimum values at 8.2 ka (Figure 2C) coinciding with the well-documented cold event [10]. This spike is also seen in the detrital parameters such as magnetic susceptibility and Ti count rate which [23] hypothesized could be due to the glacier temporarily reforming or simply cooler temperatures leading to less organic input. The average temperature optimum value of the vegetation gradually shifts colder throughout the Middle Holocene and into the Neoglacial period as Langfjordjøkelen begins to reform. Mean ground surface temperature, which can vary in proximity to a glacier, has been identified as a key explanatory variable for plant community composition in glacial forelands [47]. Similar to ground surface temperature, snow cover is also highly spatially heterogeneous and influential on vegetation composition [48]. Glaciers provide landscape obstacles for snow drift accumulation and can increase snow persistence in their immediate vicinity [49]. Thus, the change towards more cold adapted plants over the Middle and Late Holocene is likely both a direct effect of regional cooling and a local effect of an expanding glacier causing additional local cooling.

The negative correlation between plant moisture trait values and both glacial activity and annual precipitation is the opposite trend as might be intuitively expected. A greater proportion of moist-adapted plants are present during the Early and Middle Holocene when no glacier is present in the catchment (Figure 2E). Similarly, more dry-adapted plants are detected in the Late Holocene which had higher annual precipitation and is often characterized by mire and wetland formation [7,24]. The range of these average moisture trait values is fairly small (1 category: 5.1 (mesic-moist)–6.1 (moist)), but the negative correlation with glacial activity and annual precipitation is significant (Figures 4C and 5B) and could be explained by the locking-up of precipitation in both snow and ice caused by the decreasing temperatures during the Late Holocene.

The catchment of Jøkelvatnet is generally too steep for extensive mire formation, so as the Langfjordjøkel glacier melted and reformed during the Late Holocene, many of the previously mentioned species were growing on either exposed moraine ridges or in the heath directly adjacent to the lake. Additionally, it is important to note that bryophytes were excluded from all trait analyses due to poor taxonomic resolution with the gh primer set and the lack of available trait databases. While some species are highly tolerant of desiccation, bryophytes are highly dependent on locally moist conditions to propagate [50]. At Jøkelvatnet, the abundance and diversity of bryophytes were highest during the Late Holocene and for one spike at 9.3 ka (Figure 2A,B). This pattern is in contrast to that recorded by the vascular plant vegetation and offers a contradictory, and potentially more robust, view of moisture conditions around Jøkelvatnet. In addition, the pattern of moisture tolerance may not reflect overall precipitation as changes in meltwater may alter the inflow of sediments and formation of floodplains. Thus, while patterns of plant temperature optimum traits correlate well with glacial activity and the climate proxies, moisture traits may be highly impacted by the local environment and the analysis of many sites might be required to find regional patterns (e.g., [22]).

The correlation between average soil disturbance trait values and glacial activity (Figure 4A) suggests that the glacier was having a direct effect on the vegetation. Disturbance-dependent forbs such as *Oxyria digyna* and multiple *Saxifraga* species are some of the few taxa recorded in the earliest parts of the record as the valley was first becoming deglaciated. The arrival of more competitive dwarf shrubs (*Vaccinium*) and woody taxa in

zones 2 and 3 coincides with the absence of glacial activity. A similar pattern is recorded in the catchment of Lake Bolshoye Shchuchye in the Polar Urals where glaciers had nearly completely melted by 15 ka as vegetation shifted to be shrub-dominated [42,51]. In the Jøkelvatnet catchment, the increasing diversity of disturbance-dependent forbs (additional *Ranunculus* and *Saxifraga* species) during the Neoglacial period (zone 4) could be the result of increased soil erosion from the continually melting and reforming glacier during this period. In contrast, only a few small glaciers reformed in shady cirques around Lake Bolshoye Shchuchye during the Late Holocene while *Ranunculus sulphureus* and various *Saxifraga* species do not return to the sedaDNA record [42,51]. Lake Muzelle in the French Alps also displays this trend as *Saxifraga paniculata*, *Oxyria digyna*, and *Eritrichium* sp. appear towards the end of the Little Ice Age when glaciers in the catchment began to retreat [43]. Glacial activity is a good predictor of habitat availability for pioneer species [52] and the increase and arrival of these early successional stage taxa are detectable through sedaDNA.

5. Conclusions

We demonstrate that sedaDNA is a useful tool for both reconstructions of past environments and investigating changes in plant richness and composition. In particular, the more local deposition of sedaDNA compared to pollen enables a finer-scale study of how local environmental conditions may affect vegetation (e.g., the effect of a glacier on a particular catchment's flora). The sedaDNA record at Jøkelvatnet shows significant changes in the plant community at 9.7 and 4.3 ka corresponding to inflection points in Langfjordjøkel's glacial activity. A correlation of the vegetation's temperature optimum trait value with glacial activity is primarily due to climate but may have been exacerbated by a direct effect of the glacier on the plant community. Additionally the correlation of vegetation soil disturbance trait values and glacial activity implies that the glacial activity has had a direct effect on the vegetation. When compared with catchments lacking a glacier in northern Fennoscandia, Jøkelvatnet's ecosystem displays more variability throughout the Middle and Late Holocene suggesting that the Langfjordjøkel glacier has enhanced the effect of climate change on the plant community. The counterintuitive negative soil moisture trait–glacial activity relationship is likely due to a reduction in soil moisture caused by decreasing temperatures. Beyond the direct impact of climate change on arctic vegetation, our results suggest the disappearance of glaciers will have an additional effect on plant communities. Studying biotic responses to past climate change complements contemporary monitoring and field experiments when predicting the effects of current climate change on vegetation.

Supplementary Materials: The following supporting information can be downloaded at: <https://www.mdpi.com/article/10.3390/quat6010007/s1>. Figure S1. CONISS clustering based on proportions of PCR replicates. Figure S2. CONISS clustering based on proportions of total filtered reads. Figure S3. Number of PCR replicates each species appears in separated by functional group. Figure S4. Proportion of PCR replicates based on functional groups. Figure S5. Diagnostic plots for linear regressions.

Author Contributions: L.D.E., I.G.A. and A.G.B. designed the study. I.G.A., L.D.E. and L.T. did the vegetation surveys. J.B. provided access to the Jøkelvatnet core and data. D.P.R. generated the sedaDNA data. D.P.R., I.G.A. and L.D.E. matched and filtered the sedaDNA data. P.D.H. and A.G.B. provided the age-depth model. L.D.E. analyzed the data and wrote a first draft of the manuscript upon which all co-authors commented. All authors have read and agreed to the published version of the manuscript.

Funding: This work was supported by the European Research Council (ERC) under the European Union's Horizon 2020 research and innovation program grant agreement no. 819192 (to I.G.A. and A.G.B.; supported L.D.E and L.T.) for the IceAGenT project; Research Council of Norway grant 250963/F20 (to I.G.A) for the ECOGEN project.

Data Availability Statement: All data needed to evaluate the conclusions and generate the figures in the paper are present in the paper and/or the Supplementary Materials. Scripts and data used

for generating Figures 2–5 are available at (https://github.com/salanova-elliott/jokelvatnet_data (accessed on 26 September 2022)). All newly generated raw sedaDNA sequence data have been deposited in the European Nucleotide Archive (ENA) (www.ebi.ac.uk/ena/browser/home (accessed on 26 September 2022)) with BioProject accession PRJEB39329.

Acknowledgments: We would like to thank M. F. Merkel for participating in the vegetation survey and assistance with technical work; A. Reveret for comments on the manuscript; H. E. Ludwig (Wittmeier) for her previous work and providing data access; R. Paulssen and the GSCT at The Arctic University of Norway for amplicon sequencing. Bioinformatic analyses were performed on resources provided by UNINETT Sigma2—the National Infrastructure for High Performance Computing and Data Storage in Norway.

Conflicts of Interest: The authors declare no conflict of interest.

References

1. Matthews, J.A. *The Ecology of Recently-deglaciated Terrain: A Geoecological Approach to Glacier Forelands*; Cambridge University Press: Cambridge, UK, 1992; 386p.
2. Raffl, C.; Mallaun, M.; Mayer, R.; Erschbamer, B. Vegetation Succession Pattern and Diversity Changes in a Glacier Valley, Central Alps, Austria. *Arctic Antarct. Alp. Res.* **2006**, *38*, 421–428. [[CrossRef](#)]
3. Eichel, J.; Krautblatter, M.; Schmidlein, S.; Dikau, R. Biogeomorphic interactions in the Turtmann glacier forefield, Switzerland. *Geomorphology* **2013**, *201*, 98–110. [[CrossRef](#)]
4. Wojcik, R.; Eichel, J.; Bradley, J.A.; Benning, L.G. How allogenic factors affect succession in glacier forefields. *Earth-Science Rev.* **2021**, *218*, 103642. [[CrossRef](#)]
5. Romundset, A.; Akçar, N.; Fredin, O.; Tikhomirov, D.; Reber, R.; Vockenhuber, C.; Christl, M.; Schlüchter, C. Lateglacial retreat chronology of the Scandinavian Ice Sheet in Finnmark, northern Norway, reconstructed from surface exposure dating of major end moraines. *Quat. Sci. Rev.* **2017**, *177*, 130–144. [[CrossRef](#)]
6. Hughes, A.L.C.; Gyllencreutz, R.; Lohne, Ø.S.; Mangerud, J.; Svendsen, J.I. The Last Eurasian Ice Sheets—A Chronological Database and Time-Slice Reconstruction, DATED-1. *Boreas* **2016**, *45*, 1–45. [[CrossRef](#)]
7. Sjögren, P.J. An Overview of Holocene Climate Reconstructions in Northernmost Fennoscandia. SapReps. 15 February 2021. Available online: <https://septentrio.uit.no/index.php/SapReps/article/view/5747> (accessed on 1 May 2022).
8. Larocca, L.J.; Axford, Y. Arctic glaciers and ice caps through the Holocene: a circumpolar synthesis of lake-based reconstructions. *Clim. Past* **2022**, *18*, 579–606. [[CrossRef](#)]
9. Nesje, A.; Bakke, J.; Dahl, S.O.; Lie, Ø.; Matthews, J.A. Norwegian mountain glaciers in the past, present and future. *Glob. Planet. Chang.* **2008**, *60*, 10–27. [[CrossRef](#)]
10. Wanner, H.; Solomina, O.; Grosjean, M.; Ritz, S.P.; Jetel, M. Structure and origin of Holocene cold events. *Quat. Sci. Rev.* **2011**, *30*, 3109–3123. [[CrossRef](#)]
11. Birks, H.J.B. Contributions of Quaternary botany to modern ecology and biogeography. *Plant Ecol. Divers.* **2019**, *12*, 189–385. [[CrossRef](#)]
12. Sjögren, P.; Damm, C. Holocene Vegetation Change in Northernmost Fennoscandia and the Impact on Prehistoric Foragers 12 000–2000 cal. a BP—A Review. *Boreas* **2019**, *48*, 20–35. [[CrossRef](#)]
13. Sjögren, P.; van der Knaap, W.; Huusko, A.; van Leeuwen, J.F. Pollen productivity, dispersal, and correction factors for major tree taxa in the Swiss Alps based on pollen-trap results. *Rev. Palaeobot. Palynol.* **2008**, *152*, 200–210. [[CrossRef](#)]
14. Ritchie, J.C. Current trends in studies of long-term plant community dynamics. *New Phytol.* **1995**, *130*, 469–494. [[CrossRef](#)] [[PubMed](#)]
15. Alsos, I.G.; Sjögren, P.J.E.; Edwards, M.E.; Landvik, J.Y.; Gielly, L.; Forwick, M.; Coissac, E.; Brown, A.; Jakobsen, L.V.; Føreid, M.K.; et al. Sedimentary ancient DNA from Lake Skartjørna, Svalbard: Assessing the resilience of arctic flora to Holocene climate change. *Holocene* **2015**, *26*, 627–642. [[CrossRef](#)]
16. Birks, H.H.; Birks, H.J.B. Future uses of pollen analysis must include plant macrofossils. *J. Biogeogr.* 2000. Available online: <https://www.jstor.org/stable/2655981> (accessed on 14 October 2021).
17. Parducci, L.; Bennett, K.D.; Ficitola, G.F.; Alsos, I.G.; Suyama, Y.; Wood, J.R.; Pedersen, M.W. Ancient plant DNA in lake sediments. *New Phytol.* **2017**, *214*, 924–942. [[CrossRef](#)]
18. Sjögren, P.; Edwards, M.E.; Gielly, L.; Langdon, C.T.; Croudace, I.W.; Merkel, M.K.F.; Fonville, T.; Alsos, I.G. Lake sedimentary DNA accurately records 20th Century introductions of exotic conifers in Scotland. *New Phytol.* **2016**, *213*, 929–941. [[CrossRef](#)] [[PubMed](#)]
19. Taberlet, P.; Coissac, E.; Pompanon, F.; Gielly, L.; Miquel, C.; Valentini, A.; Vermet, T.; Corthier, G.; Brochmann, C.; Willerslev, E. Power and limitations of the chloroplast trnL (UAA) intron for plant DNA barcoding. *Nucleic Acids Res.* **2006**, *35*, e14. [[CrossRef](#)] [[PubMed](#)]
20. Wang, Y.; Pedersen, M.W.; Alsos, I.G.; De Sanctis, B.; Racimo, F.; Prohaska, A.; Coissac, E.; Owens, H.L.; Merkel, M.K.F.; Fernandez-Guerra, A.; et al. Author Correction: Late Quaternary dynamics of Arctic biota from ancient environmental genomics. *Nature* **2021**, *600*, 86–92. [[CrossRef](#)]

21. Tyler, T.; Herbertsson, L.; Olofsson, J.; Olsson, P.A. Ecological indicator and traits values for Swedish vascular plants. *Ecol. Indic.* **2020**, *120*, 106923. [[CrossRef](#)]
22. Alsos, I.G.; Rijal, D.P.; Ehrich, D.; Karger, D.N.; Yoccoz, N.G.; Heintzman, P.D.; Brown, A.G.; Lammers, Y.; Pellissier, L.; Alm, T.; et al. Postglacial species arrival and diversity buildup of northern ecosystems took millennia. *Sci. Adv.* **2022**, *8*, eabo7434. [[CrossRef](#)]
23. Wittmeier, H.E.; Bakke, J.; Vasskog, K.; Trachsel, M. Reconstructing Holocene glacier activity at Langfjordjøkelen, Arctic Norway, using multi-proxy fingerprinting of distal glacier-fed lake sediments. *Quat. Sci. Rev.* **2015**, *114*, 78–99. [[CrossRef](#)]
24. Karger, D.N.; Nobis, M.P.; Normand, S.; Graham, C.H.; Zimmermann, N.E. CHELSA-TraCE21k v1.0. Downscaled transient temperature and precipitation data since the last glacial maximum. *Clim. Past.* **2021**, pp. 1–27. Available online: <https://cp.copernicus.org/preprints/cp-2021-30/> (accessed on 18 May 2022).
25. Andreassen, L.M.; Winsvold, S.H.; Paul, F.; Hausberg, J.E. Inventory of Norwegian glaciers. In *Rapport*; Andreassen, L.M., Winsvold, S.H., Eds.; Norwegian Water Resources and Energy Directorate: Oslo, Norway, 2012; Volume 38, p. 240.
26. Rijal, D.P.; Heintzman, P.D.; Lammers, Y.; Yoccoz, N.G.; Lorberau, K.E.; Pitelkova, I.; Goslar, T.; Murguzur, F.J.A.; Salonen, J.S.; Helmens, K.F.; et al. Sedimentary ancient DNA shows terrestrial plant richness continuously increased over the Holocene in northern Fennoscandia. *Sci. Adv.* **2021**, *7*. [[CrossRef](#)]
27. Nesje, A. A Piston Corer for Lacustrine and Marine Sediments. *Arct. Alp. Res.* **1992**, *24*, 257. [[CrossRef](#)]
28. Blaauw, M.; Christen, J.A. Flexible paleoclimate age-depth models using an autoregressive gamma process. *Bayesian Anal.* **2011**, *6*, 457–474. [[CrossRef](#)]
29. Reimer, P.J.; Bard, E.; Bayliss, A.; Warren Beck, J.; Blackwell, P.G.; Ramsey, C.B.; Buck, C.E.; Cheng, H.; Edwards, R.L.; Friedrich, M.; et al. IntCal13 and Marine13 Radiocarbon Age Calibration Curves 0–50,000 Years cal BP. *Radiocarbon* **2013**, *55*, 1869–1887. [[CrossRef](#)]
30. Taberlet, P.; Bonin, A.; Zinger, L.; Coissac, E. *Environmental DNA: For Biodiversity Research and Monitoring*; Oxford University Press: Oxford, UK, 2018; 253p.
31. Boyer, F.; Mercier, C.; Bonin, A.; Bras, Y.L.; Taberlet, P.; Coissac, E. Obitools: A unix-inspired software package for DNA metabarcoding. *Mol. Ecol. Resour.* **2016**, *16*, 176–182. [[CrossRef](#)] [[PubMed](#)]
32. Sønstebo, J.H.; Gielly, L.; Bryisting, A.K.; Elven, R.; Edwards, M.; Haile, J.; Willerslev, E.; Coissac, E.; Rioux, D.; Sannier, J.; et al. Using next-generation sequencing for molecular reconstruction of past Arctic vegetation and climate. *Mol. Ecol. Resour.* **2010**, *10*, 1009–1018. [[CrossRef](#)] [[PubMed](#)]
33. Willerslev, E.; Davison, J.; Moora, M.; Zobel, M.; Coissac, E.; Edwards, M.E.; Lorenzen, E.D.; Vestergård, M.; Gussarova, G.; Haile, J.; et al. Fifty thousand years of Arctic vegetation and megafaunal diet. *Nature* **2014**, *506*, 47–51. [[CrossRef](#)] [[PubMed](#)]
34. Soininen, E.M.; Gauthier, G.; Bilodeau, F.; Berteaux, D.; Gielly, L.; Taberlet, P.; Gussarova, G.; Bellemain, E.; Hassel, K.; Stenøien, H.K.; et al. Highly overlapping winter diet in two sympatric lemming species revealed by DNA metabarcoding. *PLoS ONE* **2015**, *10*, e0115335. [[CrossRef](#)] [[PubMed](#)]
35. Alsos, I.G.; Lavergne, S.; Merkel, M.K.F.; Boleda, M.; Lammers, Y.; Alberti, A.; Pouchon, C.; Denoeud, F.; Pitelkova, I.; Puşcaş, M.; et al. The Treasure Vault Can be Opened: Large-Scale Genome Skimming Works Well Using Herbarium and Silica Gel Dried Material. *Plants* **2020**, *9*, 432. [[CrossRef](#)] [[PubMed](#)]
36. Elven, R.; Murray, D.F.; Razzhivin, V.Y.; Yurtsev, B.A. *Annotated Checklist of the Panarctic Flora (PAF) Vascular Plants*; Natural History Museum, University of Oslo: Oslo, Norway, 2011.
37. Elven, R.; Alm, T.; Berg, T.; Båtvik, J.I.I.; Fremstad, E.; Pedersen, O. *Johannes Lid & Dagny Tande Lid: Norsk Flora*; Det Norske Samlaget: Oslo, Norway, 2005.
38. Oksanen, J.; Blanchet, F.G.; Friendly, M.; Kindt, R.; Legendre, P.; McGlinn, D.; Minchin, P.; O'Hara, R.B.; Simpson, G.; Solymos, P.; et al. vegan: Community Ecology Package. R package version 2.5-6. Available online: <https://CRAN.R-project.org/package=vegan> (accessed on 10 March 2021).
39. Juggins, S. rioja: Analysis of Quaternary Science Data. 2020. Available online: <https://cran.r-project.org/package=rioja> (accessed on 10 March 2021).
40. Wickham, H. *Ggplot2: Elegant Graphics for Data Analysis*; Springer: New York, NY, USA, 2016; Available online: <https://ggplot2.tidyverse.org> (accessed on 10 March 2021).
41. Walker, M.D.; Walker, D.A.; Welker, J.M.; Arft, A.M.; Bardsley, T.; Brooks, P.D.; Fahnestock, J.T.; Jones, M.H.; Losleben, M.; Parsons, A.N.; et al. Long-Term Experimental Manipulation of Winter Snow Regime and Summer Temperature in Arctic and Alpine Tundra. *Hydrol. Process.* **1999**, *13*, 2315–2330. [[CrossRef](#)]
42. Clarke, C.L.; Edwards, M.E.; Gielly, L.; Ehrich, D.; Hughes, P.D.M.; Morozova, L.M.; Hafliadason, H.; Mangerud, J.; Svendsen, J.I.; Alsos, I.G. Persistence of arctic-alpine flora during 24,000 years of environmental change in the Polar Urals. *Sci. Rep.* **2019**, *9*, 1–11. [[CrossRef](#)]
43. Giguët-Covex, C.; Ficetola, G.F.; Walsh, K.; Poulenard, J.; Bajard, M.; Fouinat, L.; Sabatier, P.; Gielly, L.; Messager, E.; Develle, A.L.; et al. New insights on lake sediment DNA from the catchment: Importance of taphonomic and analytical issues on the record quality. *Sci. Rep.* **2019**, *9*, 1–21. [[CrossRef](#)]
44. Heinecke, L.; Epp, L.S.; Reschke, M.; Stoof-Leichsenring, K.R.; Mischke, S.; Plessen, B.; Herzsuh, U. Aquatic macrophyte dynamics in Lake Karakul (Eastern Pamir) over the last 29 cal ka revealed by sedimentary ancient DNA and geochemical analyses of macrofossil remains. *J. Paleolimnol.* **2017**, *58*, 403–417. [[CrossRef](#)]

45. Alsos, I.G.; Lammers, Y.; Yoccoz, N.G.; Jørgensen, T.; Sjøgren, P.; Gielly, L.; Edwards, M.E. Plant DNA metabarcoding of lake sediments: How does it represent the contemporary vegetation. *PLoS ONE* **2018**, *13*, e0195403. [[CrossRef](#)] [[PubMed](#)]
46. Ariza, M.; Fouks, B.; Mauvisseau, Q.; Halvorsen, R.; Alsos, I.G.; de Boer, H.J. Plant Biodiversity Assessment through Soil eDNA Reflects Temporal and Local Diversity. *Methods Ecol. Evol.* **2022**. [[CrossRef](#)]
47. Giaccone, E.; Luoto, M.; Vittoz, P.; Guisan, A.; Mariéthoz, G.; Lambiel, C. Influence of microclimate and geomorphological factors on alpine vegetation in the Western Swiss Alps. *Earth Surf. Process. Landforms* **2019**, *44*, 3093–3107. [[CrossRef](#)]
48. Niittynen, P.; Luoto, M. The importance of snow in species distribution models of arctic vegetation. *Ecography* **2017**, *41*, 1024–1037. [[CrossRef](#)]
49. Schuler, T.V.; Crochet, P.; Hock, R.; Jackson, M.; Barstad, I.; Johannesson, T. Distribution of snow accumulation on the Svartisen ice cap, Norway, assessed by a model of orographic precipitation. *Hydrol. Process.* **2008**, *22*, 3998–4008. [[CrossRef](#)]
50. Bates, J.W. Is “life-form” a useful concept in bryophyte ecology? *Oikos* **1998**, *82*, 223. [[CrossRef](#)]
51. Svendsen, J.I.; Færseth, L.M.B.; Gyllencreutz, R.; Hafliðason, H.; Henriksen, M.; Hovland, M.N.; Lohne, S.; Mangerud, J.; Nazarov, D.; Regnéll, C.; et al. Glacial and environmental changes over the last 60 000 years in the Polar Ural Mountains, Arctic Russia, inferred from a high-resolution lake record and other observations from adjacent areas. *Boreas* **2018**, *48*, 407–431. [[CrossRef](#)]
52. Jones, G.A.; Henry, G.H.R. Primary plant succession on recently deglaciated terrain in the Canadian High Arctic. *J. Biogeogr.* **2003**, *30*, 277–296. [[CrossRef](#)]

Disclaimer/Publisher’s Note: The statements, opinions and data contained in all publications are solely those of the individual author(s) and contributor(s) and not of MDPI and/or the editor(s). MDPI and/or the editor(s) disclaim responsibility for any injury to people or property resulting from any ideas, methods, instructions or products referred to in the content.